NASA TECHNICAL MEMORANDUM

NASA TM X-52597

NASA TM X-52597

TRANSITION FROM FILM TO NUCLEATE BOILING IN VERTICAL FORCED FLOW

by F. F. Simon and R. J. Simoneau
Lewis Research Center
Cleveland, Ohio

TECHNICAL PAPER proposed for presentation at
Eleventh National Heat Transfer Conference sponsored by the
American Society of Mechanical Engineers and the
American Institute of Chemical Engineers
Minneapolis, Minnesota, August 3-6 1969

TRANSITION FROM FILM TO NUCLEATE BOILING IN VERTICAL FORCED FLOW

by F. F. Simon and R. J. Simoneau

Lewis Research Center
Cleveland, Ohio

TECHNICAL PAPER proposed for presentation at

Eleventh National Heat Transfer Conference sponsored by the
American Society of Mechanical Engineers and the
American Institute of Chemical Engineers
Minneapolis, Minnesota, August 3-6 1969

NATIONAL AERONAUTICS AND SPACE ADMINISTRATION

TM X-52597

TRANSITION FROM FILM TO NUCLEATE BOILING IN VERTICAL FORCED FLOW

by F. F. Simon and R. J. Simoneau

Lewis Research Center
National Aeronautics and Space Administration
Cleveland, Ohio

SUMMARY

A study was made of the transition from film boiling to nucleate boiling for liquid nitrogen flowing in an electrically heated tube. For this type of heating, wall conduction is believed to govern the boiling transition. A conduction analysis was combined with a film boiling analysis for an analytical prediction of the transition heat flux. A visual experiment of film boiling aided the film boiling analysis. The analytical results are in good agreement with the experimental data.

INTRODUCTION

Little is known about the transition of film boiling to nucleate boiling in forced flow. In the study of this boiling transition, most of the attention has been directed to horizontal non-flow systems (Refs. (1-4)). Classic hydrodynamic stability theory was applied for determining the transition heat flux, (refs. (1-3)). Some experimental data of the transition heat flux in forced convection has been reported by Kutateladze and Borishanski.[5] The data reported in Ref. (5) is for water and isoproprl alcohol and shows the transition heat flux to increase with liquid velocity.

In analyzing this transition phenomenon the specification of the type of heating is important. Simon, Papell, and Simoneau[6] reported that the transition heat flux is related to whether the heating surface has a uniform heat flux (i.e., heat flux controlled) or a uniform temperature (i.e., temperature controlled). The results of Ref. (6), for nitrogen, indicate that a uniform heat flux surface will give a transition heat flux that is one order of magnitude greater than for a uniform temperature surface. Kovalev (Ref. (4)) reports a similar result for water. For this reason, this paper talks in the more broad terminology of the transition heat flux and reserves the term minimum heat flux specifically for a constant temperature system.

For the horizontal non-flow case, Zuber (Ref. (1)) successfully analyzed the minimum heat flux by applying Rayleigh-Taylor instability.[7] The essence of this approach is that an unstable vapor-liquid interface must be above the entire heating surface in order for film boiling to be sustained. In the vertical forced flow case an instability also exists; but, it is more of the Kelvin-Helmholtz type.[7] To date it has not been analyzed.

In addition to hydrodynamic instabilities another well known physical phenomenon occurs at the time of transition. On a constant heat flux surface both nucleate and film boiling can exist side by side on the heater. This was observed early in boiling work. When the two modes of boiling occur side by side, a temperature gradient exists in the heater wall. The motion of the interface between the two modes of boiling has been analyzed in terms of the conduction gradient in the uniform heat flux wall by Semeria and Martinet.[8] Koslav[4] and the authors[6] have successfully taken the approach that the transition heat flux of an electrically heated system is governed by axial conduction in the heating element. The analysis presented herein uses a conduction model and gives as one of its results the wall temperatures existing at the heating surface when transition from film boiling to nucleate boiling occurs. The wall temperature information is used in conjunction with a heat transfer analysis and experimental evidence of the nature of vertical film boiling, to develop an analysis for predicting the transition heat flux.

The first part of this paper reviews the general analytical approach to be used for predicting the transition heat flux. The second part gives the specific functions necessary to apply the general analysis to liquid nitrogen. The third section introduces new hydrodynamic and thermal information obtained from a recent visual study of vertical film boiling. This information is used in modifying the heat transfer model for the vertical film boiling of saturated, flowing liquid nitrogen. Finally, the wall conduction model analysis is compared with experimental transition heat flux data.

ANALYTIC MODEL

A boiling curve of heat flux versus the temperature difference for a given pressure and liquid velocity is shown on Fig. 1. The regions of boiling are indicated on the figure and it should be noted that a distinction is made between uniform surface heat flux and uniform surface wall temperature. The path B-E of the boiling curve is obtainable in a wall temperature controlled experiment (such as steam heating) and is unstable for a uniform wall heat flux experiment (as in electrical heating). Another difference between uniform heat flux and uniform temperature can be found in the heat flux level at which transition from film boiling to nucleate boiling occurs. References 4 and 6 report that the transition heat flux for a uniform heat flux is one order of magnitude greater than for a uniform wall temperature.

Some discussion of this difference will be made later. This investigation is limited to a uniform surface heat flux situation.

For a uniform heat flux, for the range B-E of the boiling curve, the wall temperature is not uniquely determined by the heat flux. The following three cases have been found to occur.

(1) The entire surface is in nucleate boiling at some temperature difference θ_1.

(2) The entire surface is in film boiling at some temperature difference θ_2.

(3) The surface is partially in nucleate and partially in film boiling with an axial gradient in the temperature along the surface.

Visual evidence of condition 3 was reported in Ref. (9) and is shown in Fig. 2. Condition 3 is unstable and eventually the film boiling is replaced by nucleate boiling. Investigators have reported (Refs. (10,11)) that once stable film boiling is established, a lowering of the heat flux is required (path C-D) before transition back to nucleate boiling is possible. Since a uniform heat flux permits the coexistence of film boiling and nucleate boiling (Fig. 2) a large axial temperature gradient exists between the portion of the heating surface in film boiling and in nucleate boiling. This axial gradient is believed to control the transition of film boiling to nucleate boiling because of the resulting heat flow from the section in film boiling to the section in nucleate boiling.

Anywhere along path C-D of the boiling curve (Fig. 1) axial conduction can in general be expected. However, once point D is reached, axial conduction becomes more dominating and cause the wall temperature at the leading edge of film boiling to gradually lower to a value which permits liquid wetting of the metal surface. This process may be reversed by a finite increase in heat flux above point D. The velocity of this motion is a function of the wall thermal properties and the heat flux. This is demonstrated analytically and experimentally by Semeria and Martinet (Ref. (8)). The results of Ref. (6) show that below point D the velocity of transition from film boiling to nucleate boiling increases with decreasing heat flux. This is consistent with Semeria and Martinet's results (Ref. (8)). Therefore, point D marks the heat flux level below which motion of film boiling transitioning to nucleate boiling is noted. In Semeria and Martinet's analysis the wall temperatures associated with point D were solved for by considering a zero velocity for the film boiling-nucleate boiling interface. They obtained the following relationship between the wetting temperature difference and the nucleate and film boiling temperature differences (θ_1, θ_2^* and θ_{wet} are defined on Fig. 1)

$$\theta_{wet}^2 = \theta_1 \theta_2^* \tag{1}$$

Semeria and Martinet assumed constant heat transfer coefficients for nucleate and film boiling. The authors found it necessary to utilize average heat transfer coefficients and modified Eq. (1) as follows:

$$\theta_{wet}^2 = (\theta_{1,\bar{h}})(\theta_{2,\bar{h}})^* \tag{2}$$

The wetting temperature difference is assumed to be a state property of the liquid (Ref. (12)) as follows:

$$\theta_{wet} = f_1(P, T) \tag{3}$$

The nucleate boiling temperature difference $(\theta_{1,\bar{h}})$ corresponding to the average heat transfer coefficient is a function of pressure, heat flux and liquid velocity

$$\theta_{1,\bar{h}} = f_2(P, q, \overline{U}_\ell) \tag{4}$$

Combining Eqs. (2) to (4) and solving for the average film boiling temperature difference at transition, we obtain

$$(\theta_{2,\bar{h}})^* = g(P, T, q, \overline{U}_\ell) \tag{5}$$

For transition to begin to occur, the film boiling temperature difference at the heat transfer surface must be equal to the value given by Eq. (5). The film boiling temperature difference corresponding to the average heat transfer coefficient is a function of pressure, heat flux, liquid velocity, and axial position

$$\theta_{2,\bar{h}} = f_3(P, q, \overline{U}_\ell, x) \tag{6}$$

Solution of Eqs. (5) and (6) for the transition heat flux is shown graphically in Fig. 1 by the intersection of Eqs. (5) and (6) at point D and is expressed as follows:

$$(\theta_{2,\bar{h}})^* = \theta_{2,\bar{h}};\ q_w = q_{w,T} \tag{7}$$

Equations (2) to (7) express in general, the relationship needed for a determination of the transition heat flux. However, some difficulty arises when we attempt to apply them. These equations will be applied for the case of vertical film boiling of flowing liquid nitrogen.

APPLICATION TO VERTICALLY FLOWING LIQUID NITROGEN

The model to be used for the analysis of the transition heat flux in vertical film boiling is shown in Fig. 3. The model shows an unheated entrance section and a heated section where nucleate boiling is beginning to replace film boiling. To be consistent with the physics of film boiling interfacial waves are shown in the model. An attempt will be made to take into account the effect of these waves on heat transfer.

Wetting Temperature Difference $f_1(P, T)$

Merte and Clark (Ref. (15)) in their experiments of the pool boiling of liquid nitrogen report a wetting temperature difference of 33.4° K at 1 atm. For an evaluation of the effect of pressure on the wetting temperature difference, the analysis of Spiegler, et.al. (Ref. (12)) is used. In Ref. (12) it is assumed that the wetting temperature (T_{wet}) is a state property of the fluid. The value of the wetting temperature is assumed to correspond to the maximum superheat of a fluid and this condition is determined by using Van der Waals equation of state. Spiegler found his analysis

to have good agreement with existing pool data. An additional source of data is the Leidenfrost points given for drops on page 214 of Ref. (5). The Leidenfrost point is the wetting temperature difference for drops. This data is compared with the analytical results of Ref. (12) on Fig. 5, in terms of the critical temperature and the critical pressure. Also shown in Fig. 5 are the liquid nitrogen pool boiling data points of Merte and Clark (Ref. (15)) and Ruzicka (Ref. (16)). The analysis of Spiegler, et. al. appears to represent very well the data points shown on Fig. 5.

The theoretical equation for the range of reduced pressures encountered in this study is linear and may be written as follows:

$$\frac{T_{wet}}{T_c} = 0.13\,\frac{P}{P_c} + A \tag{8}$$

The theoretical value of the constant A in Eq. (8) is 0.840. A correction is made to this constant so it conforms with the liquid nitrogen experimental evidence of Merte and Clark (Ref. (15)). The equation to be used for determination of the wetting temperature difference as a function of pressure is as follows:

$$\frac{T_{wet}}{T_c} = 0.13\,\frac{P}{P_c} + 0.872 \tag{9}$$

Average Nucleate Boiling Temperature Difference $f_2(P, q, \overline{U}_\ell)$

For determining the average nucleate boiling temperature difference in a forced flow, the method of Rohsenow (Ref. (13)) is used. The method assumes that the total heat flux may be considered as a summation of the heat flux due to boiling in the absence of flow and the heat flux due to convection in the absence of boiling

$$q_{w,1} = q_c + q_{PB} \tag{10}$$

Calculation of the pool boiling heat flux was made by using Kutaleladze's equation as reported by Brentari and Smith (Ref. (14)).

$$q_{PB} = 4.87\times10^{-7}\left(\frac{C_{p,\ell}}{\Gamma_v}\right)^{1.50}\left(\frac{k_\ell \rho_\ell^{1.282} P^{1.75}}{\sigma^{0.906}\mu_\ell^{0.626}}\right)\theta_1^{2.50} \tag{11}$$

The convection heat flux is determined by using the Dittus-Boelter equation

$$Nu = 0.024\,Re_\ell^{0.8}\,Pr_\ell^{0.4} \tag{12}$$

The computed results of Eqs. (10) to (12) are shown in Fig. 4. It is evident from Fig. 4 that for the range of liquid velocities of interest to this study, there is little effect of the convection component on the heat flux level. Thus the curves of Fig. 4 may be expressed as

$$q \approx \beta\left(\overline{U}_\ell, \frac{P}{P_c}\right)\theta_1^{2.5} \tag{13}$$

Integrating over the nucleate boiling region the average heat transfer coefficient is expressed as follows:

$$\overline{h} = \frac{\beta}{\theta_1}\int_0^{\theta_1} \tau^{1.5}\,d\tau = \frac{\beta\theta_1^{1.5}}{2.5} \tag{14}$$

The average heat transfer coefficient may also be expressed as

$$\overline{h} = \beta\theta_{1,\overline{h}}^{1.5} \tag{15}$$

Combining Eqs. (14) and (15) we obtain

$$\theta_{1,\overline{h}} = \frac{\theta_1}{1.84} \tag{16}$$

The temperature difference (θ_1) is a function of heat flux, pressure and liquid velocity and may be determined from Fig. 4.

Average Film Boiling Temperature Difference $f_3(P, q, \overline{U}_\ell, x)$

In Ref. (6) an analysis is presented for vertical laminar film boiling of a saturated, flowing liquid. The liquid-vapor interface was considered to be smooth. The analysis of Ref. (6) is summarized in Appendix A and results in the following expression relating the axial position (x) and the average wall temperature difference ($\theta_{2,\overline{h}}$)

$$\theta_{2,\overline{h}} = \frac{x}{\left[\frac{5}{4}a_1\left(\theta^4 - \theta_{wet}^4\right) + \frac{4}{3}a_2\left(\theta^3 - \theta_{wet}^3\right) + \frac{3}{2}a_3\left(\theta^2 - \theta_{wet}^2\right) + 2a_4\left(\theta - \theta_{wet}\right) + a_5 \ln\frac{\theta}{\theta_{wet}}\right]} \tag{17}$$

where the constants are listed in Appendix A.

DETAILED EXAMINATION OF FILM BOILING AT ITS LEADING EDGE

It is unlikely that Eq. (17) as it stands could accurately predict the axial temperature profile of a surface that is uniformly heated. This is clear from the visual observation of vertical film boiling reported in Ref. (9). The visual results of Ref. (9) showed that in vertical film boiling a wavy interface separates the vapor phase from the liquid phase. These waves can be noted in Fig. 2. Equation (17) assumed conduction to occur across the thickness of the vapor boundary layer. A wavy interface makes the above assumption an approximation.

The analysis and experiments of Refs. (6) and (9) suggest that major wall conduction influence occurs in the first 0.5 to 1 cm of the film boiling. Thus to complete this problem a detailed study of the leading edge of film

boiling is necessary. In Ref. (6) the location of the first thermocouple at 1.9 cm did not allow such detailed information. It was decided, therefore, to design a test section specifically to study the leading edge utilizing the flow facility of the visual experiments of Ref. (9).

Visual Experiment

This facility was a once-through liquid nitrogen system in which inlet conditions and flow rate could be controlled. The facility is described in detail in Ref. (9). Although it was a once-through facility a large supply of nitrogen made it possible to operate the rig continuously for over 2 hours allowing ample time to achieve steady conditions.

The important details of the test section are shown in Fig. 6. Several heater configurations were tried and the one shown in Fig. 6 proved the most successful. The heater geometry was of annular cross-section with the outer tube being of pyrex for viewing and the heating element being the center rod. For structural integrity the entire assembly was encased in a steel housing with viewing ports cut out. The electrical resistance heating element was a 2.54 mm O.D. by 2.04 mm I.D. by 7.6 cm long inconel tube. The inlet electrode was a brass rod of the same O.D. and was carefully fitted into the tube. The method of attachment introduced about a 0.076 cm uncertainty in the location of the leading edge, as shown in Fig. 6. A groove was cut into the electrode about 0.25 cm below the joint as a visual reference. This also served to break up the boundary layer approaching the leading edge. The uncertainty in leading edge location could be reduced for those runs in which pictures were available to determine the start of heating. Temperatures were measured by chromel-alumel thermocouples soldered to the tube and located as shown on Fig. 6. The insertion of four thermocouples into a 2.04 mm diameter tube was very difficult and the attrition rate was high. In fact, in no individual test did all the thermocouples function properly. The test section was frequently reinstrumented and the thermocouple locations were changed from time to time. The locations on Fig. 6 should be taken as typical. Data runs were repeated in order to fill in the missing points from broken thermocouples. The redundancy in some thermocouple locations served as a check on reproducibility.

The power was supplied by a 60 cycle A.C. variac.

The bulk parameters were measured quite conventionally with a platinum resistance thermometer, a bourdon tube pressure gage and a venturi flow meter. The power was measured with conventional a volt-meter and ammeter.

The visual observations were achieved with a high speed movie camera operating nominally at 5000 frames per second. The light was a 1000 watt tungsten lamp, dispersed with a frosted glass and shown through the test section from the rear.

A Modification of the Film Boiling Equation

The movies taken of the leading edge of film boiling (less than 1 cm) indicated an interface which osciallated at a frequency of the order of 1000 cycles per second. The interface oscillated between a high value of the film thickness which will be called the peak thickness (δ_P – see Fig. 3) to a lower value of the thickness which is labeled the valley thickness (δ_V). This oscillating interface sweeps through a portion of the vapor thickness that might otherwise be a part of the energy conduction path between the vapor liquid interface and the wall. A simple film boiling model which attempts to take into account the oscillating interface is shown in Fig. 3. Figure 3 shows a mixing region created by the oscillating interface and a laminar region in which conduction is assumed to occur. The idea of a mixing region was conceived by Hsu and Westwater (Ref. (17)) in their study of turbulent film boiling. The mixing region can be expected to go beyond the amplitude of oscillation. Because of this, the laminar thickness (δ_L) should be less than the value of the valley thickness (δ_V). The laminar thickness is expressed as a fraction of the average film thickness

$$\epsilon = \frac{\delta_L}{\bar{\delta}} \tag{18}$$

An estimate of the fraction of the vapor thickness in a laminar condition can be made from the high speed movies made of film boiling. Two conditions were chosen for obtaining film thickness and wave amplitude data. These conditions are listed in table I. The variable believed to have the greatest influence on the interfacial waves is the liquid velocity. This is demonstrated visually in Fig. 7. Figure 7 shows prints from the high speed movies, from which the data for table I were determined. The two prints correspond to a liquid velocity of 1.1 m/sec and a higher velocity of 2.5 m/sec. Figure 7 demonstrates what was generally noted that the wave length will decrease and the wave amplitude will increase with increased liquid velocity. The results of wave amplitude and film thickness measurements for the conditions of Fig. 7 are listed in table I. By assuming the average film thickness to be the average of the peak thickness (δ_P) and the valley thickness (δ_V), a simple relationship is obtained for the fraction of the vapor thickness which is in laminar flow

$$\epsilon = \frac{\delta_L}{\bar{\delta}} = \frac{\delta_L}{\delta_V}\left(1 - \frac{a}{2\bar{\delta}}\right) \tag{19}$$

The work of Glenn Coury (Ref. (17)) gives a similar result by a different appraoch. His result can be stated as follows:

$$\epsilon = \left(1 - \left(\frac{a}{\bar{\delta}}\right)^2\right)^{1/2} \tag{20}$$

The values of the amplitude to thickness ratio ($a/\bar{\delta}$) reported here (table I) are in the range of ratios calculated by Coury from heat transfer considerations. Since the valley thickness (δ_V) is greater than or equal to the laminar thickness (δ_L) it is assumed that these two thicknesses are equal for the purpose of computing the film thickness ratio (ϵ) from Eq. (19) and the hydrodynamic data of table I. The result of the computation is shown in table I. We next wish to see how the hydrodynamic calculation of the thickness ratio (ϵ) compares with analysis and the measured wall temperature profiles. Equation (19) modifies Eq. (A8) as follows

$$\bar{\delta} = \frac{\bar{k}_v \theta}{\epsilon q_w} \tag{21}$$

Use of Eq. (21) in the subsequent equations of Appendix A results in the following modifications to the coefficients of Eq. (17).

$$a_1' = \frac{a_1}{\epsilon^3},\ a_2' = \frac{a_2}{\epsilon^3},\ a_3' = \frac{a_3}{\epsilon^3},\ a_4' = \frac{a_4}{\epsilon},\ a_5' = \frac{a_5}{\epsilon}$$

A comparison of the modified version of the profile Eq. (A12) is made with the experimental temperature profiles of the leading edge of film boiling. The comparison is shown in Fig. 8 for various values of the film thickness ratio (ϵ). It is clear in Fig. 8 that a film thickness ratio, ϵ, of one is not realistic. This was expected from the visual evidence of the film boiling. Figure 8 shows that the film thickness ratio (ϵ) vaires with the liquid velocity. The value of the ratio varies from 0.7 at a liquid velocity of 1.0 m/sec to 0.3 at a velocity of 2.5 m/sec. This change of the film thickness ratio with liquid velocity is consistent with the change noted in the hydrodynamic measurements. Table I shows the amplitude of interfacial oscillation to be greater for the higher liquid velocity. This results in a decrease in the calculated value of the film thickness ratio with increase in liquid velocity as shown in table I. However, the variation of the film thickness ratio with velocity as shown in table I is not as great as the variation which is needed to be consistent with the experimental data (Figs. 8(a) to (c)). The value of the film thickness ratio calculated from the hydrodynamic data is slightly larger. This is to be expected since in the wave calculation it was assumed that the valley thickness (δ_V) was equal to the laminar thickness (δ_L). This is consistent with the model, Fig. 3, which assumes the oscillating interface will influence the region beyond the wave valley position.

The film thickness ratio may be thought of as a correction to the film boiling analysis of Ref. (6) (Eq. 17). The variation of the film thickness ratio with velocity may be a result of the analysis not being complete in comprehending the physics of film boiling or it may be the result of the velocity effect on the interfacial waves shown in Fig. 7. For calculation purposes this paper restricts itself to a film thickness ratio (ϵ) of 0.5 because of the incomplete knowledge of the effect of liquid velocity and pressure on this parameter.

Laminar-Turbulent Transition

A boundary condition in the derivation by Semeria and Martinet of Eq. (1) was a zero axial conduction at an infinite distance from the leading edge of film boiling and nucleate boiling ($x = \pm\infty$). Therefore, the temperatures of Eq. (1), (θ_1 and θ_2^*), are for an infinite distance from the leading edge where the conduction gradient is zero. Calculation of the nucleate boiling temperature difference for use in Eq. (2) presented no problem. The film boiling heat-transfer analysis presented herein is for a laminar model and yields an increasing wall temperature with distance x, or a heat-transfer coefficient which decreases with distance. In reality this laminar film will eventually transition to a turbulent film. Once transition to turbulent film boiling occurs, the analytical results of Hsu and Westwater (Ref. (18)) show an increase in the heat-transfer coefficient. Based on this information once the vapor film becomes turbulent, the boiling mechanism is more efficient and axial conduction gradient no longer has a significant effect on the wetting mechanism.

Figure 9 demonstrates by the matching of the three runs, the temperature profile obtained from the electrically heated rod (Fig. 6). The surface temperature increases until a distance of 1 cm from the start of film boiling, where the wall temperature shows a nearly constant value and in some cases a decrease. This flattening of the temperature profile after 1 cm can be attributed to the transition of laminar film boiling to turbulent film boiling. This transition is fortunate because it permits a limiting value to the high wall temperatures encountered in film boiling. Visual evidence of the transition to turbulent film boiing was reported in Ref. (9) and is shown in Fig. 10. Shown in Fig. 10 are individual frames taken from high speed movies (5000 frames per sec) made of the view of an electrically heated vertical strip. Because the pictures shown on Fig. 10 were taken at the transition heat flux, the replacement of film boiling can be noted. In the film boiling region a wave instability can be seen. This can also be seen in two frames of the high speed movies taken of the heated tube described in this paper (Fig. 11). In Fig. 10 instability is noted at a distance of 0.38 cm and in Fig. 11 at a distance of 0.36 cm. The transition from laminar to turbulent film boiling is probably gradual as shown by the temperature profile of Fig. 9.

Effective Conduction Length

It is apparent from the temperature profile data that conduction is no longer effective after a distance of one cm. The equation for the effective conduction length is developed in Appendix A. Using the new film boiling data presented herein the coefficient in Eq. (A18) has been recomputed.

$$Le = 2.38 \sqrt{\frac{k_m t \theta_{2,\bar{h}}}{q_w}} \tag{22}$$

COMPARISON OF ANALYTICAL TRANSITION HEAT FLUX RESULTS WITH EXPERIMENT

A detailed description of the experimental apparatus and the procedure used for determining the transition heat flux of liquid nitrogen is given in Ref. (6). Essentially the experimental approach was to force liquid nitrogen at the saturation point through an instrumented, electrically heated test section. The test section was a nickel alloy tubing with an I.D. of 1.28 cm, a wall thickness of 0.025 cm, and a heated length of 30.5 cm. Once film boiling was established at a given liquid flow and pressure level, the power to the test section was gradually reduced. For each increment of power reduction sufficient time was allowed (approx $1\frac{1}{2}$ min) to note the appearance of nucleate boiling at the first thermocouple station (x = 1.90 cm). Nucleate boiling would begin to appear at a small increment of heat flux below the transition heat flux. The transition heat flux was taken as the lowest power level that allowed film boiling to exist over the entire heating surface.

Comparison of the analytical prediction of the transition heat flux with the experimental data is shown in Fig. 12 for three pressure levels. Figure 12 shows a reasonable quantitative agreement between theory and experiment. Particularly encouraging is that the analysis yields the proper influence of velocity on the transition heat flux at all pressure levels. Cross plotting the data of Fig. 12 against pressure for various velocities indicates that the pressure trends predicted by theory are not completely consistent with the data. However, since some of the numbers involved herein change drastically with pressure (e.g., θ^2_{wet} changes approx one order of magnitude over the pressures of this experiment) the analytic prediction is considered correct to the first order. Because of the many assumptions involved in the entire analysis it is difficult to place a finger on the exact source of the problem. The most likely candidate, however, is the computation of θ_{wet} from such a simple equation of state as Van der Waals. To illustrate this the values of T_{wet}/T_c necessary to make the data correlate perfectly are compared to Eq. (9) on Fig. 13. From Fig. 13 it can be seen that a very small error in computing T_{wet}/T_c can account for the pressure discrepancies.

Finally the analysis of Semeria and Martinet gives only the ultimate equilibrium condition but now how rapidly this equilibrium condition is reached. Thus the transition heat flux obtained experimentally could be lower than predicted because the experimentor did not wait long enough at a higher heat flux for transition to occur. For discussion on transition rates see Ref. (6).

ADDITIONAL INFORMATION ON THE INFLUENCE OF THE WALL ON TRANSITION

This study has considered the transitions from film boiling to nucleate boiling that is caused by axial conduction in the heating element. Kovalev (Ref. (4)) says that this type of transition occurs at what he calls "the equilibrium heat flux." Kovalev states what is demonstrated in Fig. 1 that the equilibrium heat flux occurs between the maximum heat flux and the minimum heat flux. He reports experiments for the film boiling of water in a pool which show the difference between the equilibrium heat flux and the minimum heat. His experiments were done with an electrically heated wire. To prevent cooling of the ends of the wire Kovalev allowed the ends to be slightly exposed to superheated vapor. In this way he eliminated conduction effects and was able to obtain the minimum heat flux. The authors performed a similar type of experiment by additional heating at the entrance of the tubular test section. This prevented conduction effects and allowed the heat flux to be lowered below the transition heat flux to a value close to the pool minimum heat flux for liquid nitrogen reported by Merte and Clark.[15] In the experiments of Kovalev, the transition heat flux was obtained by not exposing the wire ends which then permitted a conduction gradient at the wire ends.

Simon, Papell and Simoneau reported (Ref. (6)) that the transition heat flux in a heat flux controlled system is one order of magnitude greater than in a temperature controlled system. In a constant temperature system the minimum heat flux is controlled by the surface temperature difference (θ_{wet}) at which wetting of the surface occurs. This was evident in the experiments of Koslav (Ref. (4)) where an increase in the wettability of the surface by the liquid resulted in an increase in the minimum heat flux. For a heating surface with electrical heat generation, the transition to nucleate boiling depends on the conduction gradient and the surface wettability. Wall conduction transfers heat from the film boiling side to the nucleate boiling side and causes the surface temperature to drop as a function of time. Transition from film boiling to nucleate boiling gradually occurs when the wall temperature at each position along the heating surface reaches the wetting temperature.

CONCLUSIONS

The transition from film boiling to nucleate boiling in an electrically heated system appears to be governed by wall conduction. The wall conduction model of Semeria and Mertinet was used for obtaining the wall temperatures associated with the transition heat flux. These wall temperatures were used in conjunction with a heat transfer analysis for an analytical prediction of the transition heat flux. Analysis and experiment were in agreement especially in predicting the positive change of the transition heat flux with liquid velocity.

Based on hydrodynamic and wall temperature information it was found that the film boiling heat transfer analysis required modification. Visual evidence of vertical film boiling in the region of the leading edge shows a wavy, vapor-liquid interface which oscillates at a fairly high frequency. By using measurements of the oscillating interface an attempt was made at modifying a heat transfer analysis which assumed no vapor-liquid oscillation. Information of the wall temperature profile provided a direct method of modifying the heat transfer analysis. The wall temperature profile at the leading edge of film boiling shows a laminar to turbulent film boiling transition. This is consistent with visual evidence which indicates a change at the vapor-liquid interface from stable to unstable waves.

Pool data shows the transition heat flux for a uniform surface heat flux (heat flux controlled) to be one order of magnitude higher than for heating with a uniform surface temperature (temperature controlled). This difference is attributed to the wall conduction which exists for a uniform heat flux and which is not present for a uniform wall temperature.

The authors wish to thank Dr. Y. Y. Hsu for his technical advice.

SYMBOLS

A constant, dimensionless

a wave amplitude, $\delta_p - \delta_v$, cm

b $\overline{k}/\overline{T}$, W/(m)(^{o}K)

C_o $\overline{\rho k}$, (kg)(W)/(m^4)(^{o}K)

C_p specific heat, J/(kg)(^{o}K)

D tube diameter, cm

g acceleration of gravity, 9.8 m/sec^2

h heat-transfer coefficient, q/θ, $W/(m^2)(^oK)$

k thermal conductivity, $W/(m)(^oK)$

Le effective length, cm

N superheat constant, dimensionless

Nu Nusselt number, $h_\ell D/k_\ell$, dimensionless

P pressure, N/m^2

Pr Prandtl number, $C_p\mu/k$, dimensionless

q heat flux, W/m^2

Re Reynolds number, $\overline{U}_\ell D_\ell \rho_\ell / \mu_\ell$, dimensionless

T temperature, ^oK

t wall thickness, cm

U x component of velocity, m/sec

V y component of velocity, m/sec

v volume, m^3

W mass flow rate, kg/(m)(sec)

x distance along heating surface, cm

y distance away from heating surface, cm

α thermal diffusivity, $k/\rho C_p$, m^2/sec

β intercept

Γ heat of vaporization, J/kg

Γ' effective heat of vaporization, J/kg

δ film thickness, cm

ϵ film thickness ratio, $\delta_L/\overline{\delta}$

θ temperature difference, $(T_w - T_{sat})$, ^oK

μ viscosity, $(N)(sec)/m^2$

ρ density; k/m^3

σ surface tension, N/m

Subscripts:

C convection

c critical

$\overline{h}$ variable is evaluated at conditions corresponding to average heat-transfer coefficient

L Laminar

ℓ liquid

m metal

min minimum

P peak

PB pool nucleate boiling, $U_\ell = 0$

s saturation

T transition

V valley

v vapor

w wall

wet wetting

1 nucleate boiling side

2 film boiling side

Superscripts:

– average quantity

* transition film boiling condition

' modified film boiling conditions

APPENDIX - FILM BOILING ANALYSIS

The film boilng analysis is made assuming the following conditions applicable.

(1) Laminar, two dimensional vapor flow
(2) Uniform wall heat flux
(3) Linear temperature profile across the vapor film
(4) Inertia terms neglected
(5) Greater velocity gradient in the y direction than the velocity gradient in the x direction, $\partial U/\partial y >> \partial U/\partial x$
(6) Slug flow velocity profile in the liquid stream
(7) Liquid at the saturation temperature
(8) Evaluation of vapor properties across the vapor film at the average temperature of the wall and the saturated liquid, $\overline{T}(x) = (T_w(x) + T_s)/2$
(9) Constant heat capacity and Prandtl number

The basic equation relating the heat transfer at the wall and the vapor generation at the vapor-liquid interface is

$$q_w = \Gamma' \frac{dW}{dx} \qquad (A1)$$

where

$$\Gamma' = \Gamma + NC_{p,v}\theta(x) \tag{A2}$$

and

$$W = \overline{U}_v \overline{\rho}_v \overline{\delta}$$

(Average conditions are for a fixed position x.) In this analysis, the superheat constant is taken as N = 0.5.

Based on assumptions (4), (5), and (8), the momentum equation for vertical boiling may be given as

$$0 = -\frac{\partial P}{\partial x} - \overline{\rho}_v g + \overline{\mu}_v \frac{\partial^2 U_v}{\partial_y 2} \tag{A4}$$

and

$$\frac{\partial P}{dx} = -\rho_\ell g \tag{A5}$$

The applicable boundary conditions are

$$U_v = \overline{U}_\ell;\ y = \overline{\delta}$$

$$U_v = 0;\ y = 0$$

Solution of Eq. (A4) for the boundary conditions given, and subsequent integration across the vapor film yields an average velocity

$$\overline{U}_v = \frac{g(\rho - \overline{\rho}_v)}{12\mu_v}\overline{\delta}^2 + \frac{\overline{U}_\ell}{2} \tag{A6}$$

Since $\rho_\ell >> \overline{\rho}_v$, the average velocity is simply

$$\overline{U}_v = \frac{g\rho_\ell \overline{\delta}^2}{12\overline{\mu}_v} + \frac{\overline{U}_\ell}{2} \tag{A7}$$

From assumption (4) the film thickness $\overline{\delta}$ may be expressed in terms of the temperature difference $\theta(x)$ as

$$\overline{\delta} = \frac{k_v \theta}{q_w} \tag{A8}$$

When it is assumed that the thermal conductivity vaires directly with temperature, the product of the vapor density ρ_v and the thermal conductivity k_v, for an ideal gas is constant ($\rho_v k_v = C_o$). With this assumption Eqs. (A1), (A2), and (A3) can be combined with Eq.s (A7) and (A8) to yield

$$q_w = (\Gamma + NC_{p,v}\theta)\frac{d}{dx}\left(\frac{g\rho_\ell C_o C_{p,v}}{12q_w^3 Pr_v}\overline{k}_v\theta^3 + \frac{\overline{U}_\ell C_o}{2q_w}\theta\right) \tag{A9}$$

Everything in the brackets to be differentiated with respect to x can be considered constant except the thermal conductivity $\overline{k}_v$ and the temperature difference θ.

Expressing the thermal conductivity $\overline{k}_v$ as

$$\overline{k} = b\overline{T} \tag{A10}$$

and carrying out the differentiation of Eq. (A13) with respect to x results in the following equation

$$q_w = (\Gamma + NC_{p,v}\theta)\left[\frac{g\rho_\ell C_o}{12q_w^3}\frac{C_{p,v}}{Pr_v} b\left(2\theta^3 + 3\theta^2 T_s\right) + \frac{\overline{U}_\ell C_o}{2q_w}\right]\frac{d\theta}{dx} \tag{A11}$$

Equation (A11) may be integrated directly by separation of variables to yield

$$x = a_1\left(\theta^5 - \theta_{wet}^5\right) + a_2\left(\theta^4 - \theta_{wet}^4\right) + a_3\left(\theta^3 - \theta_{wet}^3\right) + a_4\left(\theta^2 - \theta_{wet}^2\right) + a_5\left(\theta - \theta_{wet}\right) \tag{A12}$$

where

$$a_1 = \frac{2}{5}\frac{A_o NC_{p,v}}{q_w^4}$$

$$a_2 = \frac{A_o}{q_w^4}\left(\frac{\Gamma}{2} + \frac{3T_s N}{4}C_{p,v}\right)$$

$$a_3 = \frac{A_o \Gamma T_s}{q_w^4}$$

$$a_4 = \frac{C_o \overline{U}_\ell NC_{p,v}}{4q_w^2}$$

$$a_5 = \frac{C_o \overline{U}_\ell \Gamma}{2q_w^2}$$

$$A_o = \frac{g\rho_\ell C_o C_{p,v} b}{12Pr_v}$$

and

$$C_o = \overline{\rho}_v \overline{k}_v = \rho_v k_v$$

The average film-boiling heat-transfer coefficient at any point x is defined as

$$h = \frac{\int_0^x h dx}{\int_0^x dx} = \frac{q}{x}\int_0^x \frac{1}{\theta}dx \tag{A13}$$

The average heat-transfer coefficient is also used to define $\theta_{2,\overline{h}}$

$$\overline{h} = \frac{q_w}{\theta_{2,\overline{h}}} \tag{A14}$$

Therefore from Eqs. (A18) and (A19), the equation for the film boiling temperature difference based on the average heat-transfer coefficient $\theta_{2,\overline{h}}$ is

$$\theta_{2,\bar{h}} = \frac{x}{\left[\frac{5}{4}a_1\left(\theta^4 - \theta_{wet}^4\right) + \frac{4}{3}a_2\left(\theta^3 - \theta_{wet}^3\right) + \frac{3}{2}a_3\left(\theta^2 - \theta_{wet}^2\right) + 2a_4\left(\theta - \theta_{wet}\right) + a_5 \ln\frac{\theta}{\theta_{wet}}\right]} \qquad \text{(A15)}$$

The conduction gradient for film boiling existing in the region where nucleate and film boiling coexist can be obtained from the analysis of Semeria and Martinet by differentiating Eq. (3.8) of Ref. (8).

$$\frac{d\theta}{dx} = (\theta_{2,\bar{h}} - \theta_{wet})\left(\frac{\bar{h}_2}{k_m t}\right)^{1/2} \exp\left[-\left(\frac{\bar{h}_2}{k_m t}\right)^{1/2} x\right] \qquad \text{(A16)}$$

The film temperature difference $\theta_{2,\bar{h}}$ is based on the average heat-transfer coefficient evaluated over the effective length Le. This evaluation makes the resulting expression implicit and requires an iterative solution.

The effective conduction length Le is determined when the conduction gradient becomes effectively too small to influence the region where nucleate boiling is gradually replacing film boiling. This may be expressed as a fractional change:

$$\frac{\left(\frac{d\theta}{dx}\right)_{x=Le}}{\left(\frac{d\theta}{dx}\right)_{x=0}} = \exp\left[-\left(\frac{\bar{h}_2}{k_m t}\right)^{1/2} Le\right] = Z \qquad \text{(A17)}$$

The data for the calculation of the fractional conduction change (Z) from Eq. (A17) was taken from Fig. 10. This is because Fig. 10 represents conditions existing at the transition heat flux. The effective conduction length is assumed to occur at the position where the interfacial waves first become unstable (x = 0.38 cm). This is believed to mark the beginning of transition to turbulent film boiling. In Ref. (6) the analytical expression for $\theta_{2,\bar{h}}(x)$ (Eq. (A15)) was applied for determining the average heat transfer coefficient in Eq. (A17). The values used in Ref. (6) for Eq. (A17) are as follows:

$$\bar{h}_2 = \frac{6.52\times10^4 \text{ W/m}^2}{282^\circ \text{ K}} = 231 \text{ W/(m}^2)(^\circ\text{K})$$

$$Le = 3.8\times10^{-3} \text{ m}$$

$$k_m = 9.7 \text{ W/(m)}(^\circ\text{K})$$

$$t = 1.02\times10^{-4} \text{ m}$$

The value obtained for Z is Z = 0.16, indicating, according to Eq. (A17), that the conduction gradient has diminished to 16 percent of its initial value at x = 0. For the purpose of determining the effective conduction length at other conditions, a constant value of Z is assumed which results in the following equation for the effective conduction length:

$$Le = 1.86\sqrt{\frac{k_m t \theta_{2,\bar{h}}}{q_w}} \qquad \text{(A18)}$$

REFERENCES

1. N. Zuber, "On the Stability of Boiling Heat Transfer," Transactions of the ASME, vol. 80, no. 3, April, 1958, pp. 711-720.

2. P. J. Berenson, "Film-Boiling Heat Transfer from a Horizontal Surface," Journal of Heat Transfer, vol. 83, no. 3, August, 1961, pp. 351-358.

3. J. H. Lienhard and P. T. Y. Wong, "The Dominant Unstable Wavelength and Minimum Heat Flux During Film Boiling on a Horizontal Cylinder," Journal of Heat Transfer, vol. 86, no. 2, May, 1964, pp. 220-226.

4. S. A. Kovalev, "An Investigation of Minimum Heat Fluxes in Pool Boiling of Water," International Journal of Heat and Mass Transfer, vol. 9, 1966, pp. 1219-1226.

5. S. S. Kutateladze and V. M. Borishanskii (J. B. Arthur, trans.), A Concise Encyclopedia of Heat Transfer, Pergamon Press, New York, N.Y., 1966, pp. 212-214.

6. F. F. Simon, S. S. Papell, and R. J. Simoneau, "Minimum Film-Boiling Heat Flux in Vertical Flow of Liquid Nitrogen," NASA TN D-4307, 1968.

7. S. Chandrasekhar, Hydrodynamic and Hydromagnetic Stability, Clarendon Press, Oxford, England, 1961.

8. R. Semeria and B. Martinet, "Calefaction Spots on a Heating Wall, Temperature Distribution and Resorption," presented at the Institute of Mechanical Engineers Symposium on Boiling Heat Transfer in Steam Generating Units and Heat Exchangers, Manchester, England, September 15-16, 1965.

9. R. J. Simoneau and F. F. Simon, "A Visual Study of Velocity and Buoyancy Effects on Boiling Nitrogen," NASA TN D-3354, 1966.

10. J. P. Lewis, J. H. Goodykoontz, and J. F. Kline, "Boiling Heat Transfer to Liquid Hydrogen and Nitrogen in Forced Flow," NASA TN D-1314, 1962.

11. R. S. Dougall and W. M. Rohsenow, "Film Boiling on the Inside of Vertical Tubes with Upward Flow of the Fluid at Low Qualities," Massachusetts Institute of Technology Report TR-9079-26, September, 1963.

12. P. Spiegler, J. Hopenfeld, M. Silberberg, C. F. Bumpus, Jr., and A. Norman, "Onset of Stable Film Boiling and the Foam Limit," International Journal of Heat and Mass Transfer, vol. 6, 1963,

pp. 987-994.

13. W. M. Rohsenow and H. Y. Choi, Heat, Mass, and Momentum Transfer, Prentice-Hall, Inc., Englewood Cliff, N.J., 1961, p. 226.

14. E. G. Brentari and R. V. Smith, "Nucleate and Film Pool Boiling Design Correlations for O_2, N_2, H_2, and He," Internationa Advances in Cryogenic Engineering, Vol. 10, Plenum Press, New York, N.Y., 1965, pp. 325-341.

15. H. Merte, Jr. and J. A. Clark, "Boiling Heat Transfer with Cryogenic Fluids at Standard, Fractional, and Near-Zero Gravity," Journal of Heat Transfer, vol. 86, no. 3, August, 1964, pp. 351-359.

16. J. Ruzicka, "Heat Transfer to Boiling Nitrogen," Problems of Low-Temperature Physics and Thermodynamics, Pergamon Press, New York, N.Y., 1959, pp. 323-329.

17. G. Goury, "A Study of Vertical Turbulent Film Boiling and Interfacial Effects," University of Houston, Ph.D. Thesis, 1968.

18. Y. Y. Hsu and J. W. Westwater, "Approximate Theory for Film Boiling on Vertical Surfaces," Chemical Engineering Progress Symposium Series, vol. 56, no.30, 1960, pp. 15-24.

Reduced pressure, P/P_c	Average liquid velocity, $\overline{U}_\ell$, m/sec	Heat flux, q_w, W/m^2	Peak film thickness, δ_P, cm	Valley film thickness, δ_V, cm	Amplitude, a, cm	Average film thickness, $\overline{\delta}$, cm	Predicted film thickness, $\overline{\delta}$, cm (Eqs. (A8) and (A12))	Amplitude to measured thickness ratio, $a/\overline{\delta}$	Position, x, cm	Thickness ratio, $\epsilon = \delta_L/\overline{\delta}$
0.087	1.1	11×10^4	0.036	0.022	0.014	0.029	0.022	0.45	0.35	0.78
0.089	2.5	20	0.043	0.020	0.023	0.033	0.031	0.70	0.33	0.65

TABLE I RESULTS OF FILM THICKNESS MEASUREMENTS

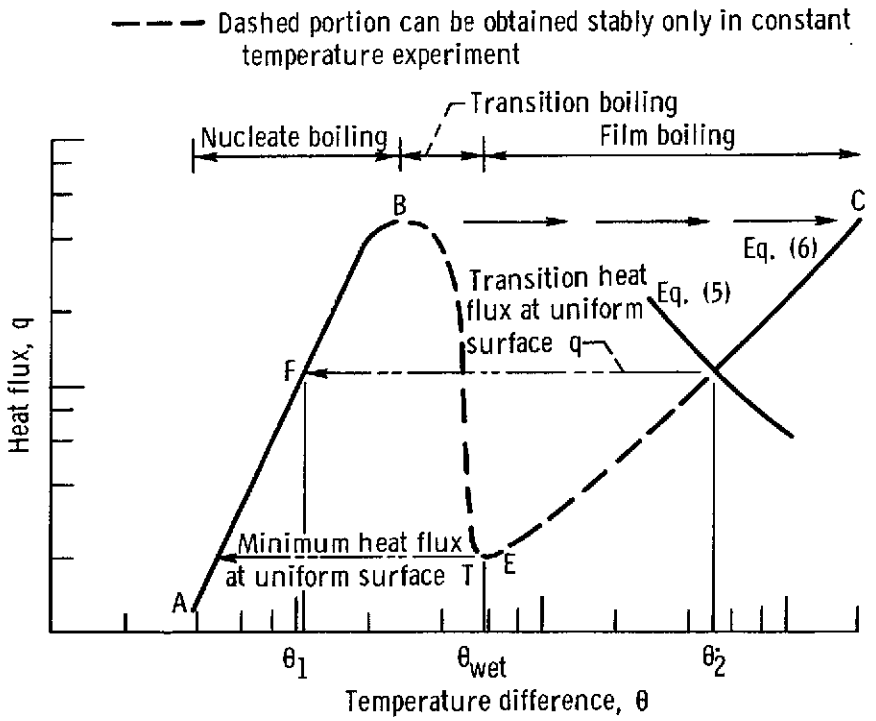

Figure 1. - Boiling curve.

//

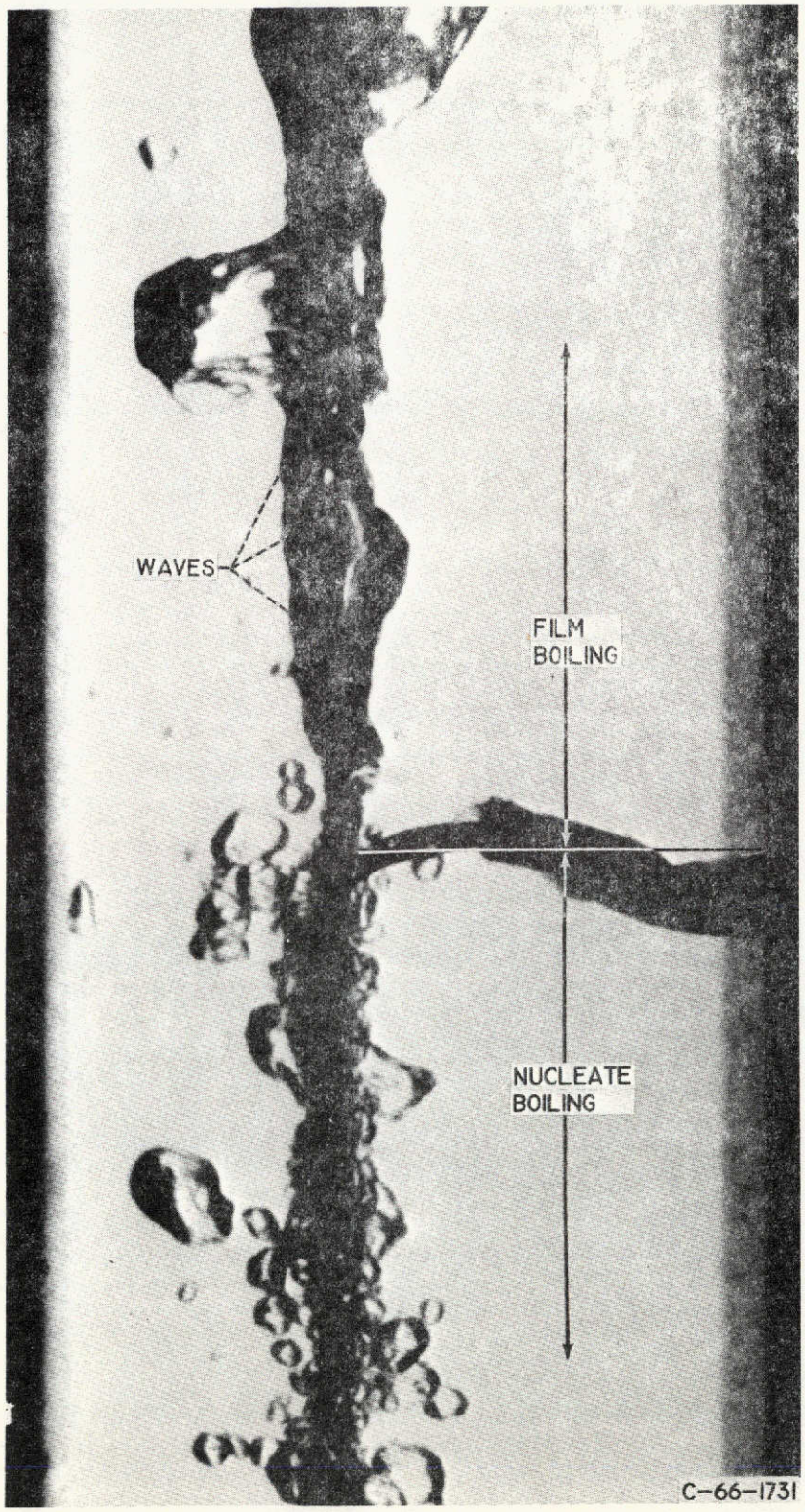

Figure 2. - Nucleate transition region in vicinity of transition heat-flux (upward flow). Velocity, 0.27 m/sec; heat flux, 6.9×10^4 w/m^2.

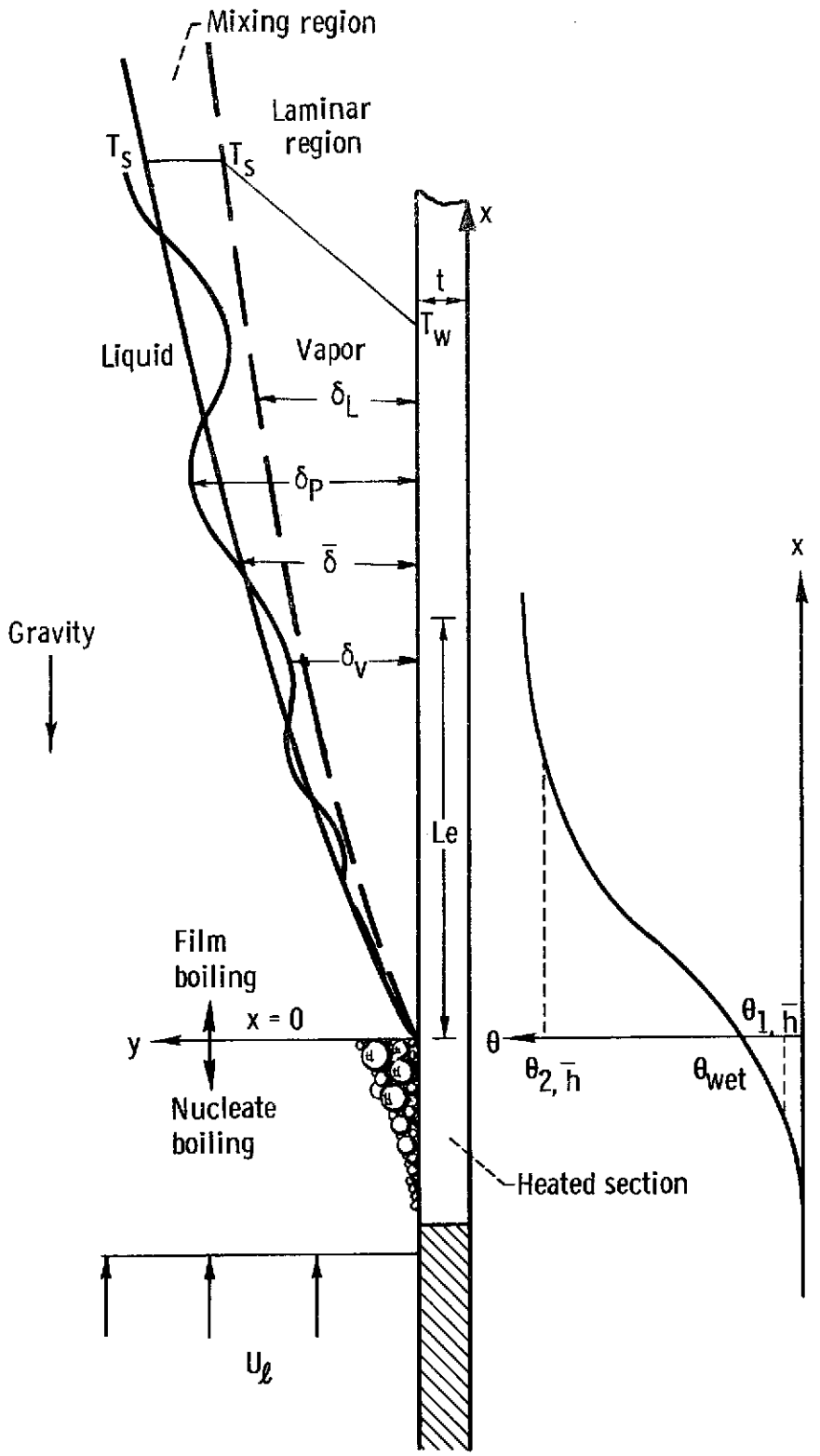

Figure 3. - Film boiling model.

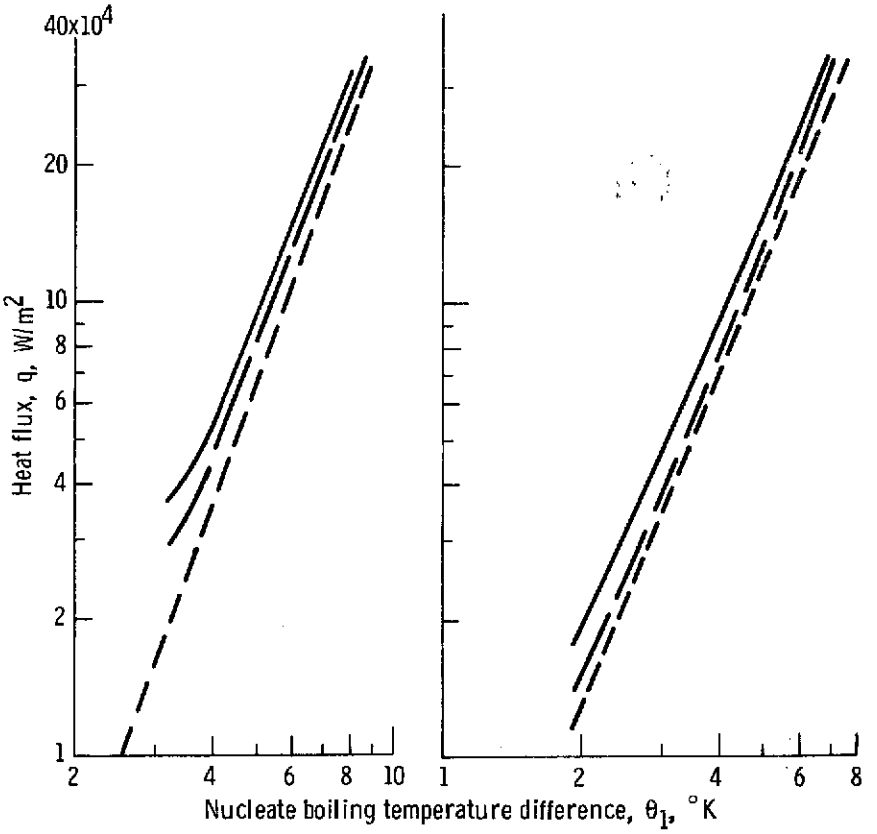

(a) Reduced pressure, 0.071. (b) Reduced pressure, 0.20.

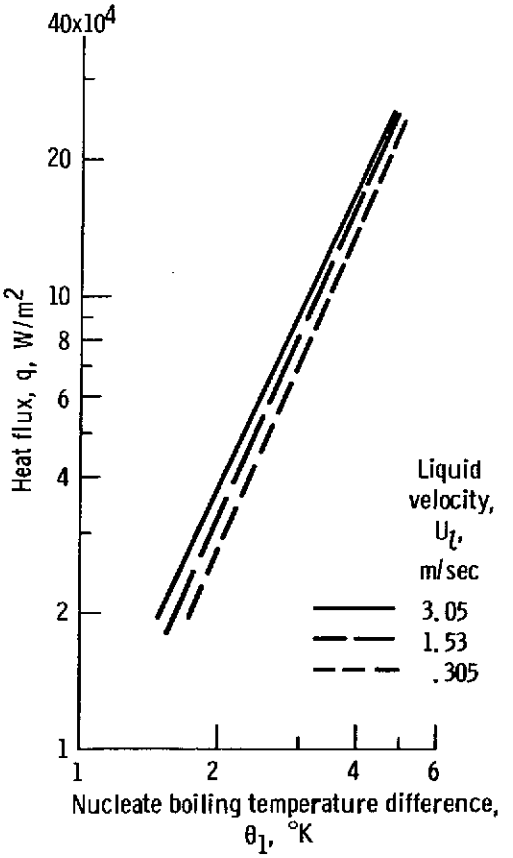

(c) Reduced pressure, 0.40.

Figure 4. - Nucleate boiling heat flux as function of temperature difference.

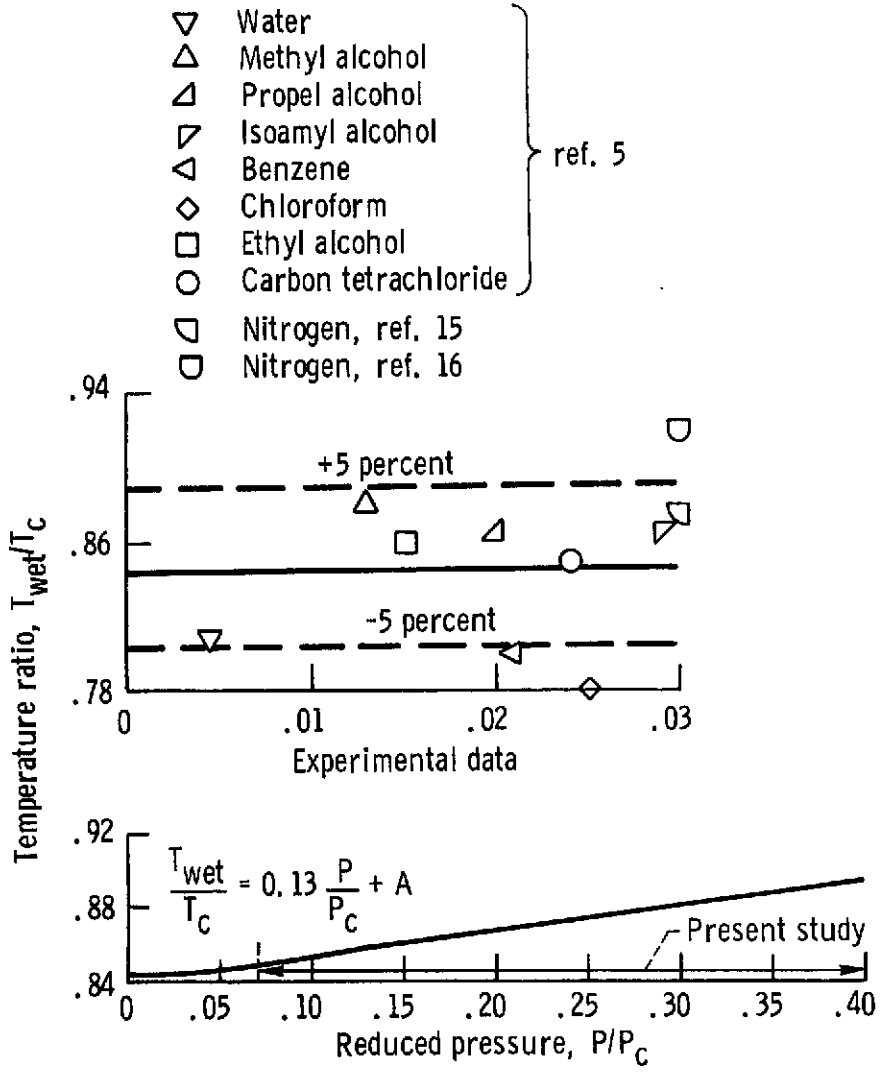

Figure 5. - Theoretical determination of wetting temperature from reference 12.

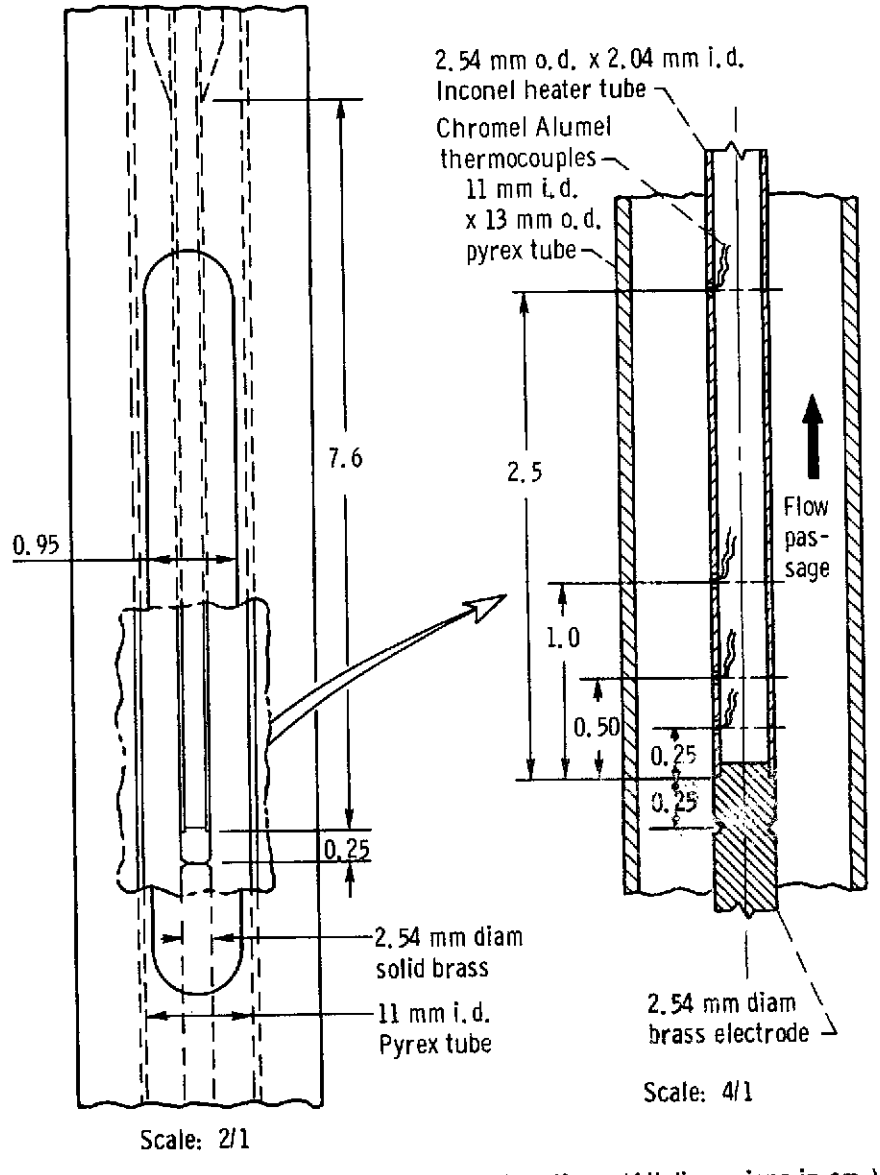

Figure 6. - Leading edge of film boiling - test section. (All dimensions in cm.)

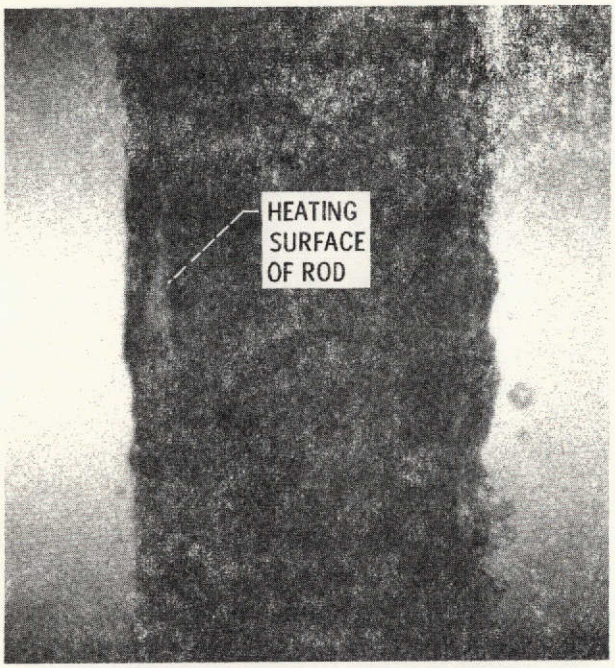

Liquid velocity, 1.1 m/sec; heat flux, 11×10^4 w/m^2.

Liquid velocity, 2.5 m/sec; heat flux, 20×10^4 w/m^2.

Figure 7. - Film boiling at the leading edge of a 2.54 mm diameter vertical rod.

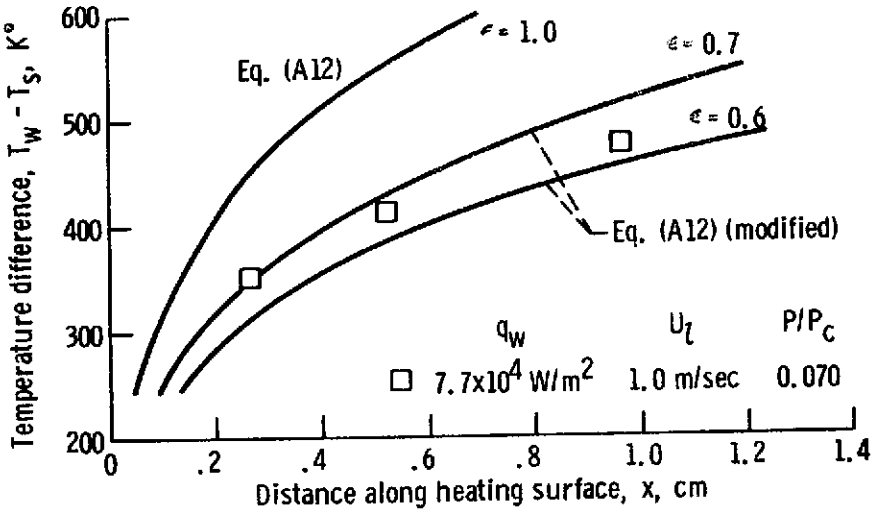

(a)

Figure 8. - Comparison of experimental temperature profile with analysis in the region of the leading edge of film boiling for values of the film thickness ratio (ϵ).

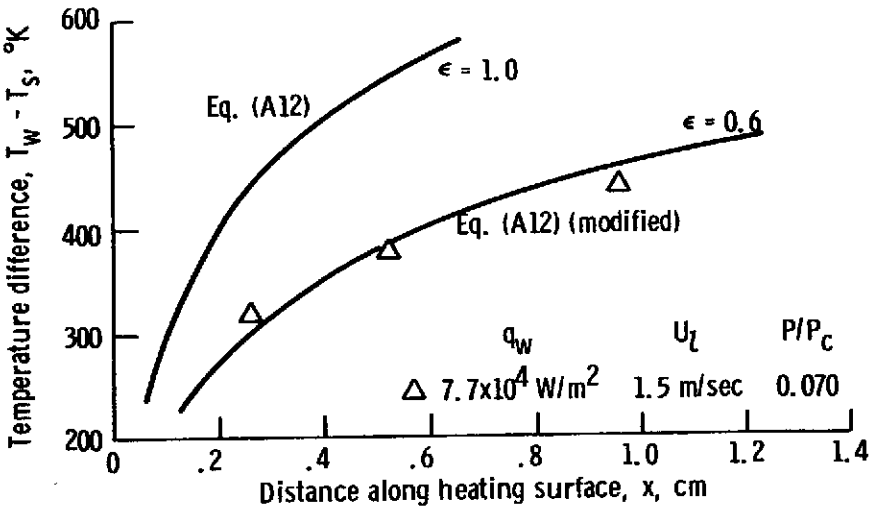

(b)

Figure 8. - Continued.

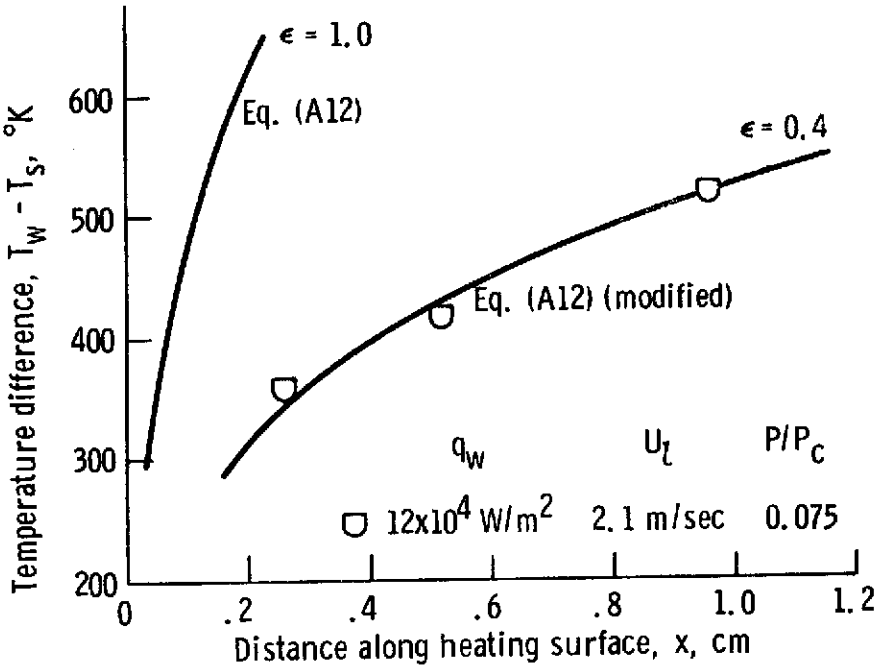

(c)

Figure 8. - Continued.

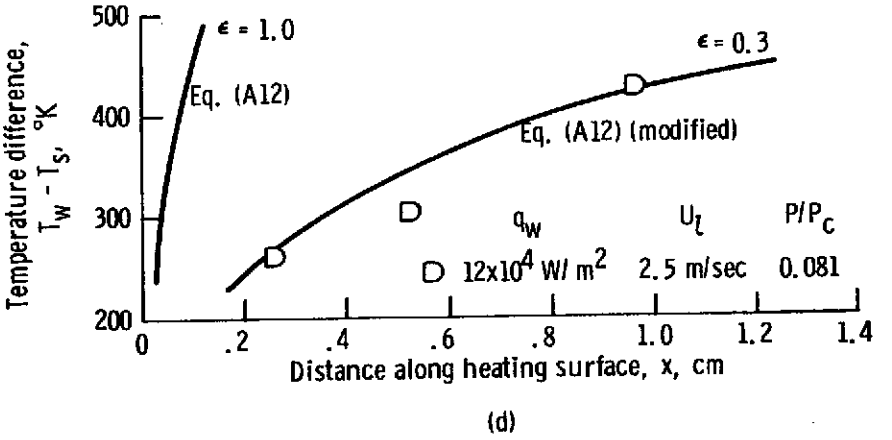

(d)

Figure 8. - Concluded.

E-4930

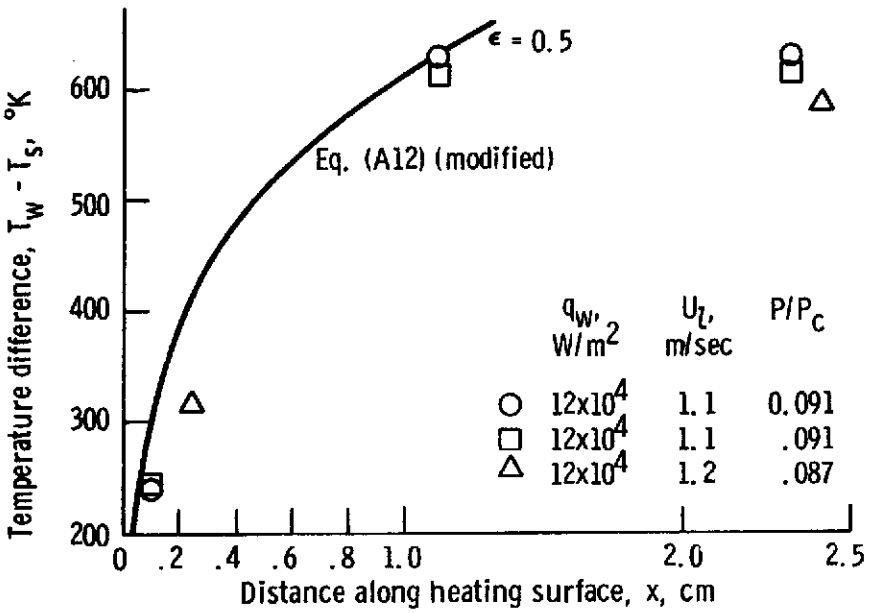

Figure 9. - Temperature profile in the region of the leading edge of vertical film boiling.

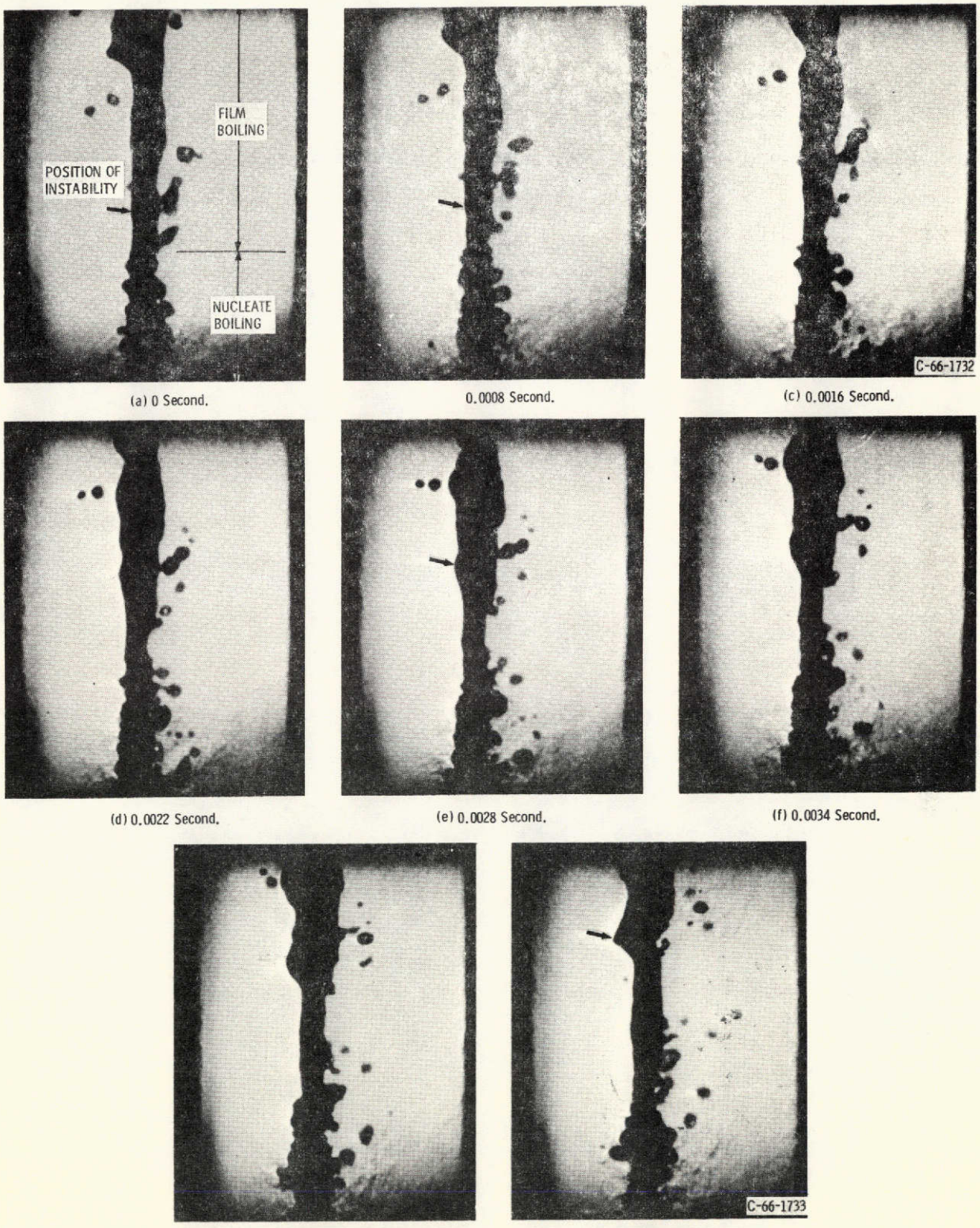

(a) 0 Second.

0.0008 Second.

(c) 0.0016 Second.

(d) 0.0022 Second.

(e) 0.0028 Second.

(f) 0.0034 Second.

(g) 0.0042 Second.

(h) 0.0054 Second.

Figure 10. - Coexistence of nucleate and film boiling in region of transition heat flux. Velocity, 0.76 meter per second; heat flux, 6.52×10^4 watts per square meter.

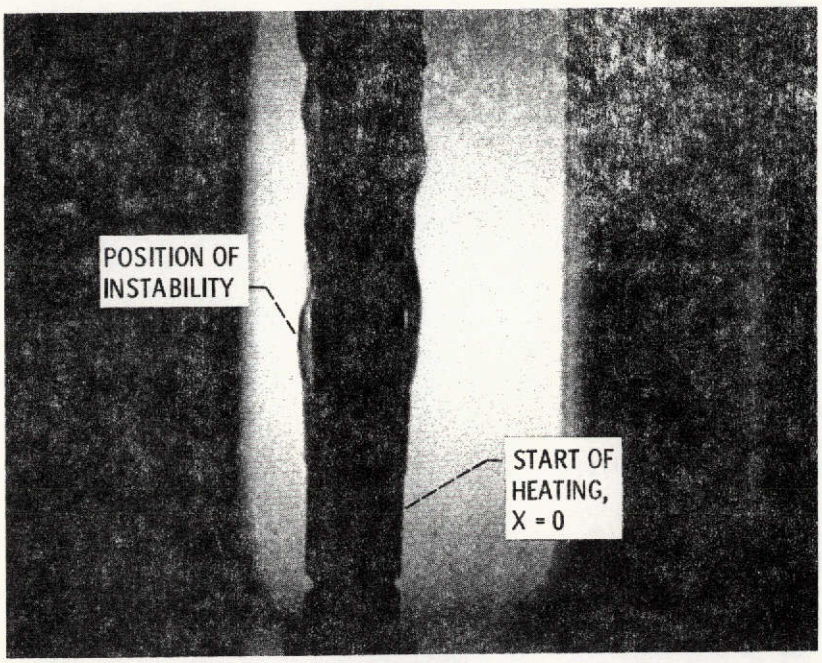

0 second

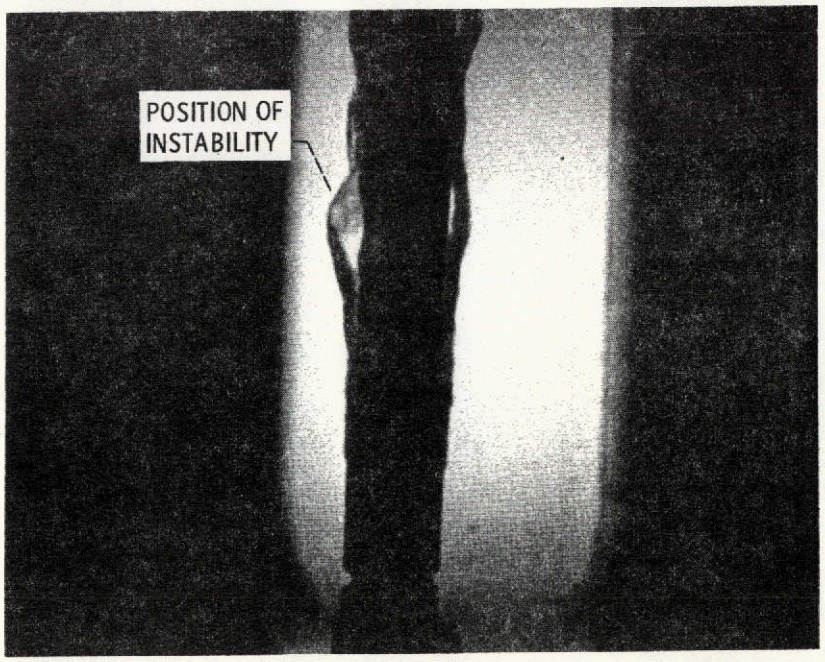

0.003 second

Figure 11. Film boiling on a vertical rod (D = 2.54 mm). Liquid velocity, 1.1 m/sec; heat flux, 11×10^4 w/m^2.

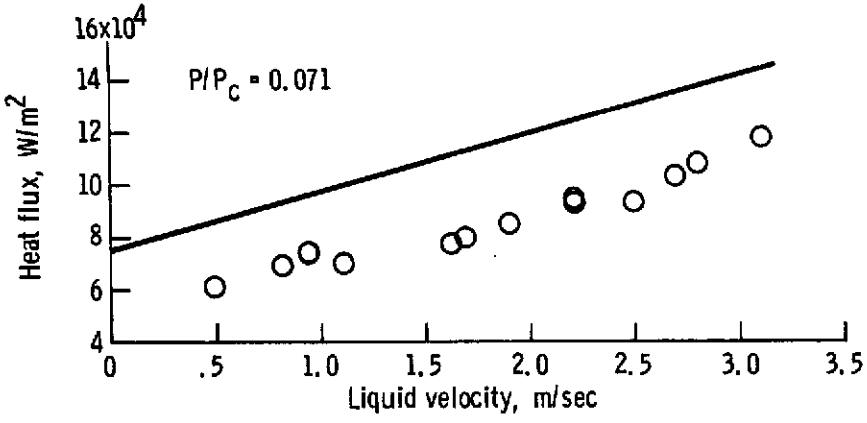

(a)

Figure 12. - Transition heat flux as a function of average liquid velocity.

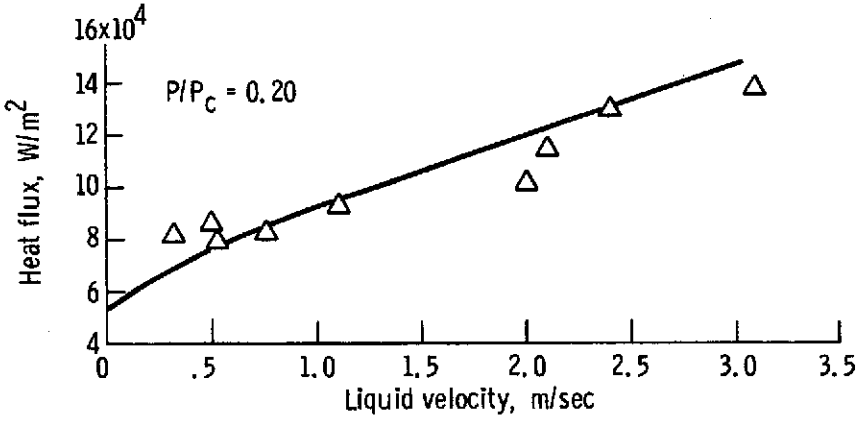

(b)

Figure 12. - Continued.

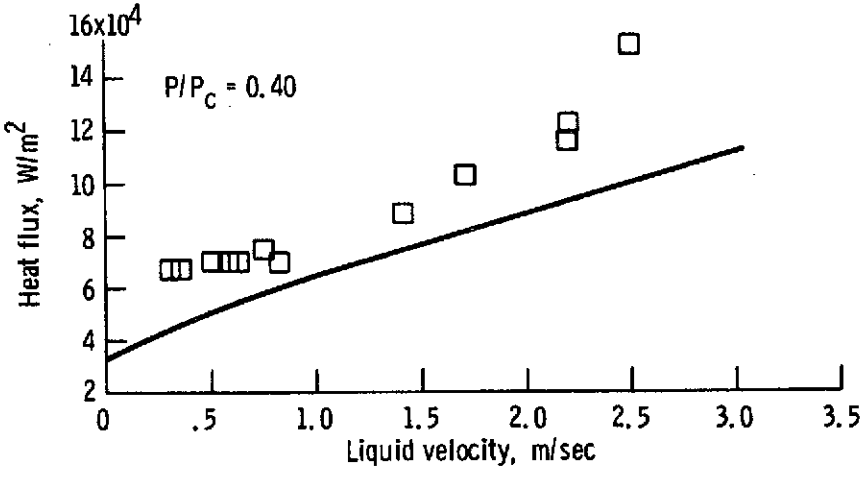

(c)

Figure 12. - Concluded.

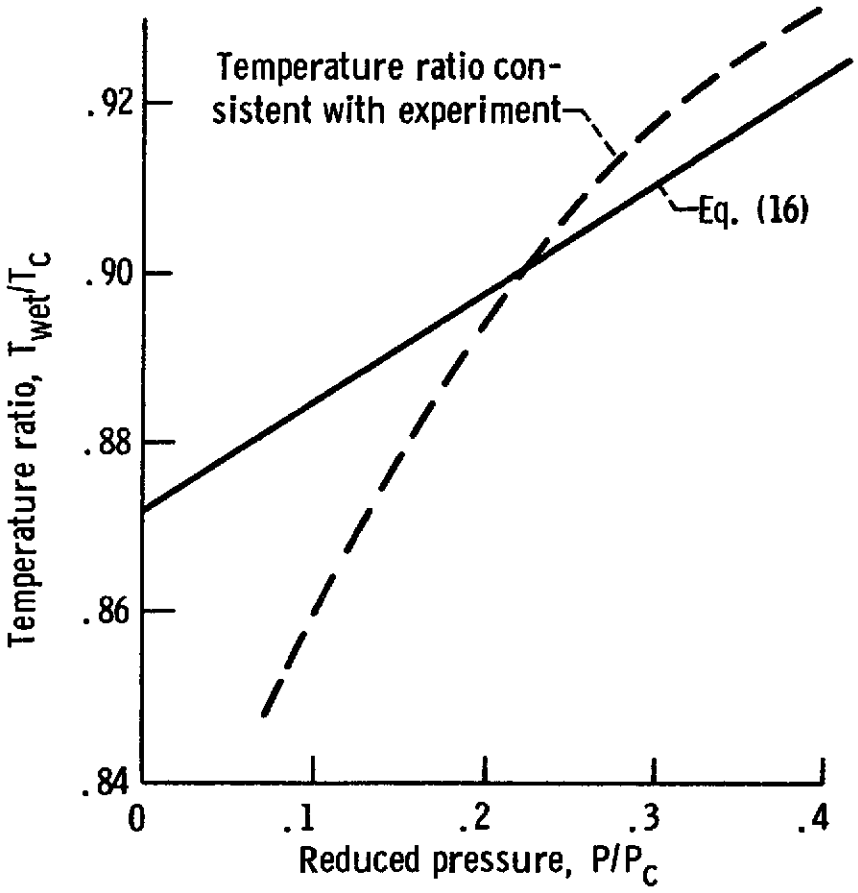

Figure 13. - Comparison of equation (16) with the temperature ratio consistent with experiment.

NASA-CLEVELAND, OHIO E-4930